

ALMA Memo 381

Elements for E-Plane Split-Block Waveguide Circuits

A. R. Kerr
5 July 2001

E-plane split-block waveguide construction is well suited to many millimeter-wave components, including power dividers, frequency multipliers, and single-ended, balanced and sideband-separating mixers [1]. Recent ALMA memos have described quadrature hybrids [2] and a matched power divider [3] suitable for split-block construction. This memo describes four additional waveguide elements which can be used as building blocks in more complex circuits: a compact H-plane bend, a short E-plane bend, a matched E-plane Y-junction, and a broadband transducer from full-height waveguide to quartz suspended stripline. The components are suitable for fabrication on a CNC milling machine using an end-mill of diameter equal to the waveguide height, and do not require the insertion of separate waveguide short-circuit pieces at the ends of waveguides. Prototype designs are given for WR-10 waveguide (75-110 GHz), which can be scaled for any other waveguide size with the same 2:1 aspect ratio.

1. H-Plane Waveguide Bend

A split-block H-plane waveguide bend allows coupling from a waveguide in the plane of the split to a waveguide perpendicular to the plane of the split. Such a bend allows waveguide circuits on different planes to be interconnected, thereby making complex circuits more compact. Two H-plane bends are described here, one with both waveguides of rectangular cross section, and the other with an oval waveguide perpendicular to the plane of the joint. These are shown in Figs. 1 and 2, with their characteristics as simulated by QuickWave [4], and with measurements for comparison in Fig. 1. Figures 3 and 4 show the dimensions of the two designs. In the first design, the rectangular waveguide perpendicular to the plane of the split can be fabricated as a cylindrical insert and pressed or soldered into the upper half of the block prior to machining the rest of the waveguide in that half. In the second design, the oval waveguide can be machined directly into the block with an end-mill, but the length of the oval waveguide is limited by the length of the milling cutter.

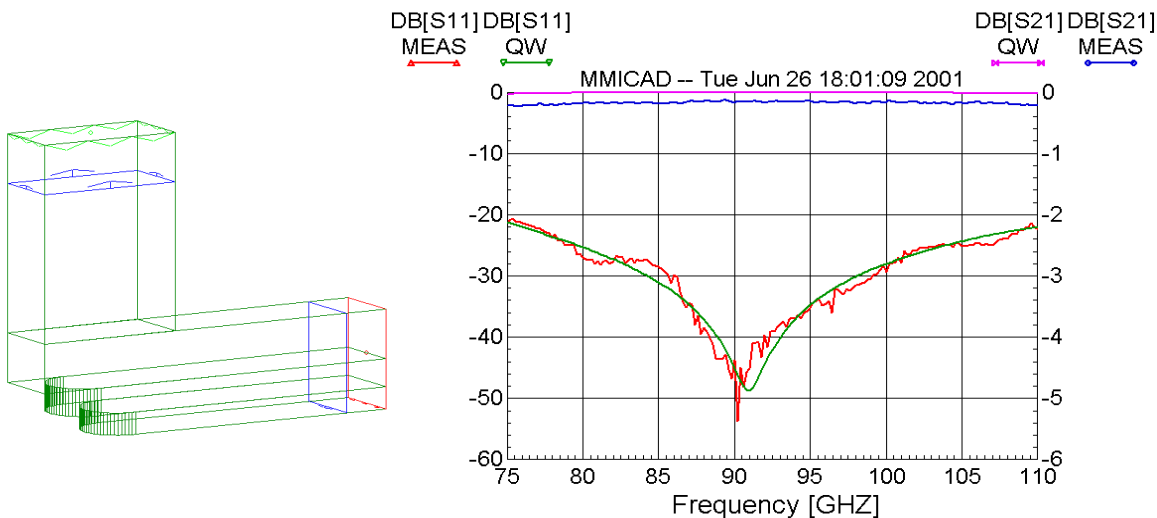


Fig. 1. WR-10 H-plane bend with rectangular waveguides. QuickWave simulation and measured |S11| and |S21| (dB).

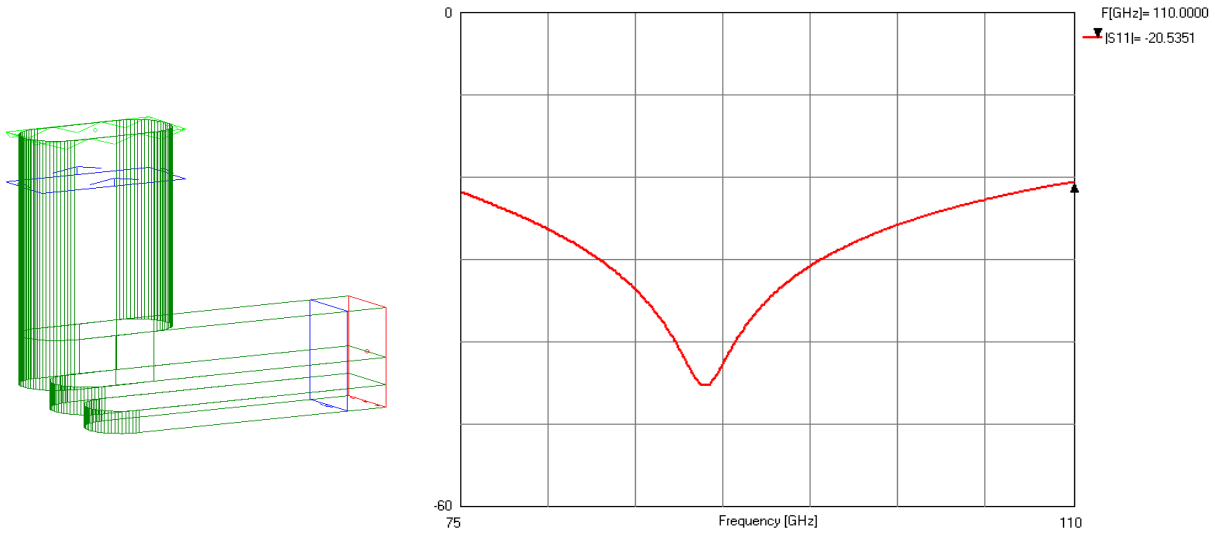


Fig. 2. WR-10 H-plane bend with an oval upper waveguide. QuickWave simulation of $|S_{11}|$ (dB).

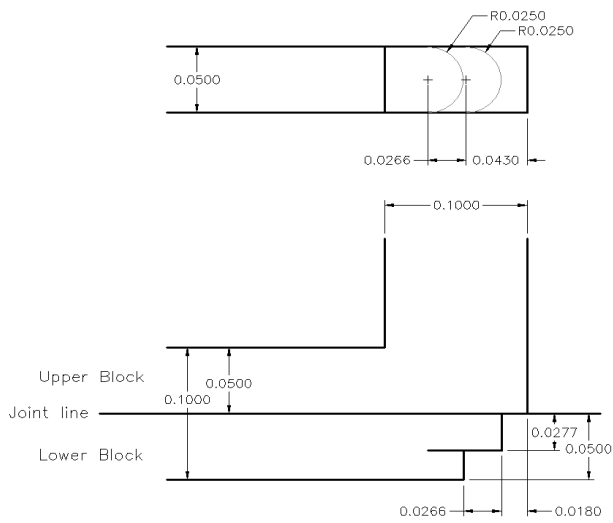


Fig. 3. H-plane bend with rectangular waveguides.

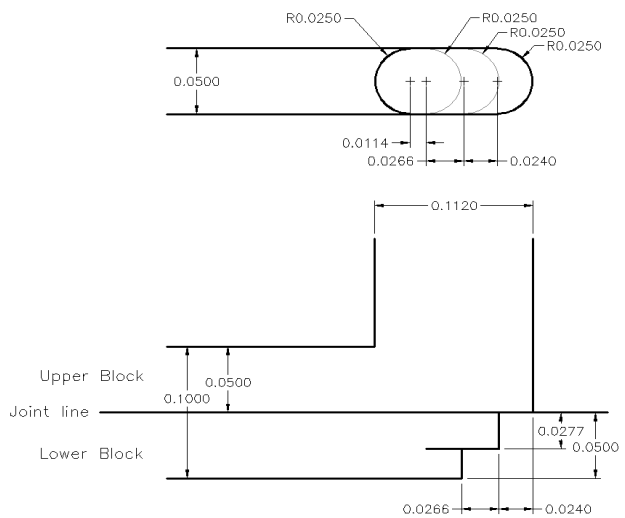


Fig. 4. H-plane bend with an oval upper waveguide.

2. E-Plane Bends

A family of simple 90° E-plane bends allows SWR to be traded against compactness. Figures 5-8 show results simulated using QuickWave for WR-10 bends with inside radii 0.020", 0.030", 0.040" and 0.060". Further increase of radius reduces $|S_{11}|$, but as $|S_{11}| < -37$ dB across the full waveguide band for the 0.060" bend, there is probably little need for E-plane bends of larger radius.

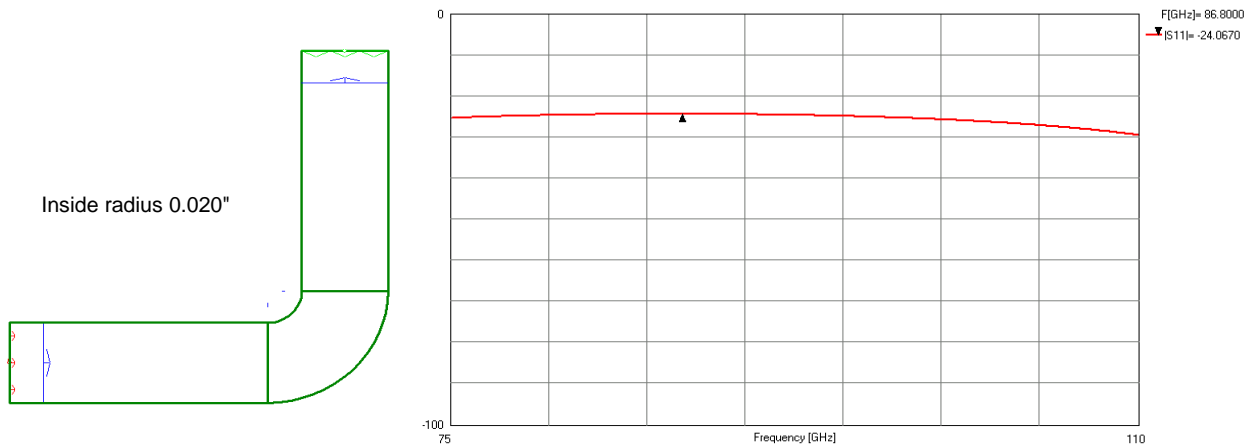


Fig. 5. WR-10 E-plane bend with inside radius 0.020". QuickWave simulation of $|S_{11}|$ (dB).

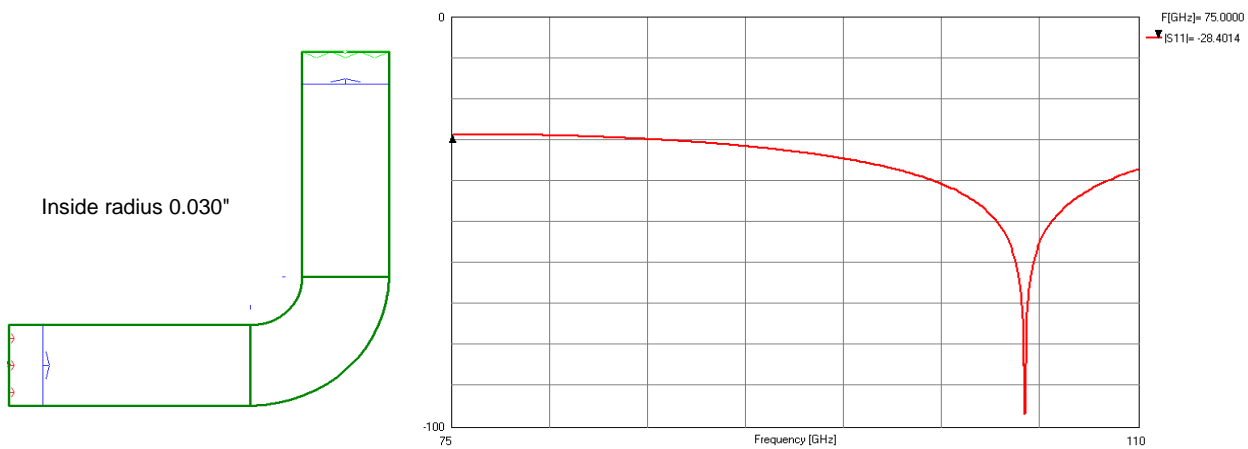


Fig. 6. WR-10 E-plane bend with inside radius 0.030". QuickWave simulation of $|S_{11}|$ (dB).

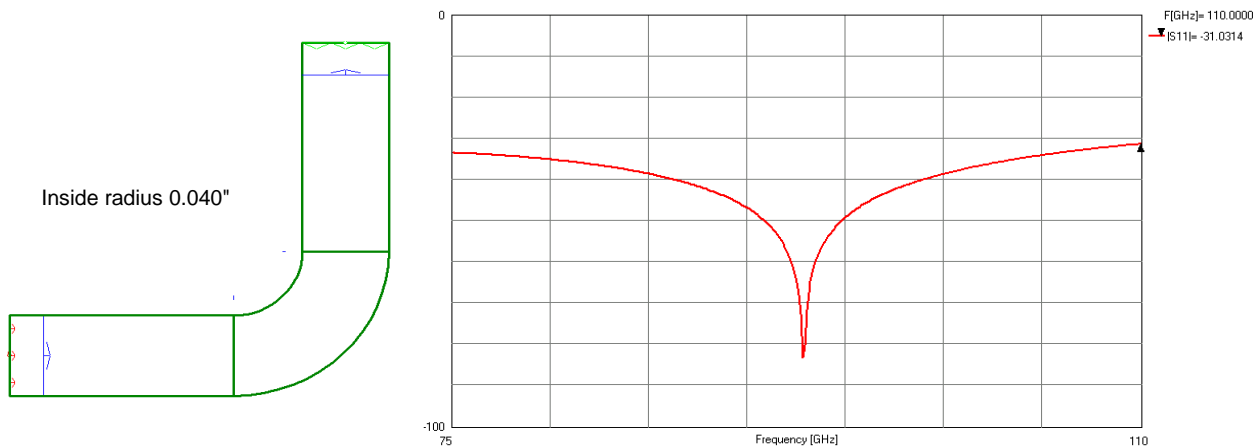


Fig. 7. WR-10 E-plane bend with inside radius 0.040". QuickWave simulation of $|S_{11}|$ (dB).

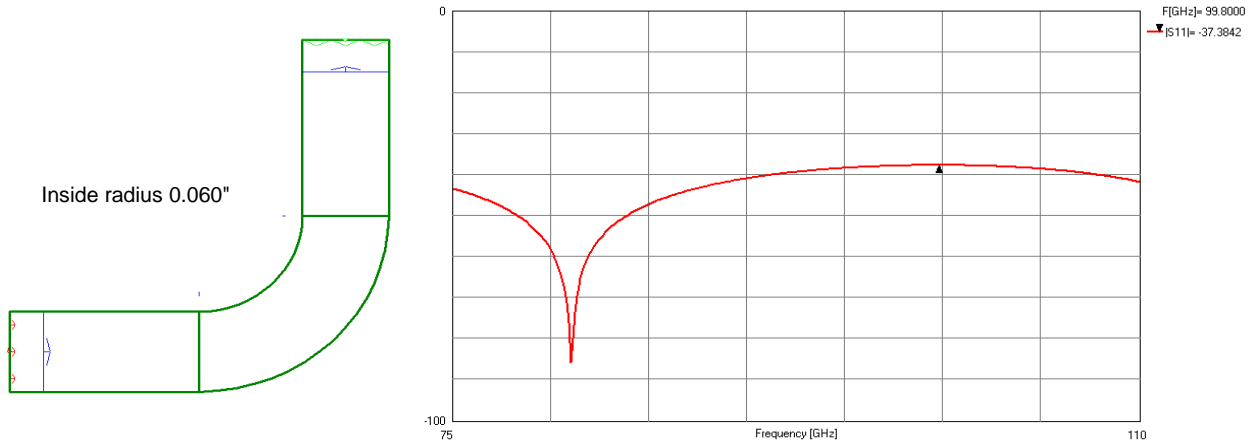


Fig. 8. WR-10 E-plane bend with inside radius 0.060". QuickWave simulation of $|S_{11}|$ (dB).

3. E-Plane Y-junction

E-plane Y-junctions are useful as power dividers and combiners in situations in which the more complex 4-port 180° hybrid (magic-T) [3] is not required. Two matched Y-junctions are described here, version A in which the cusp at the junction of the curved waveguide arms is truncated at a width of 0.0020" (see Figs. 9 and 11), and version B in which the cusp is truncated at 0.0057" (see Figs. 10 and 12). The latter design is more suitable for scaling to frequencies above ~ 300 GHz. The design procedure was as follows: The 3-section transformer from rectangular-to-square waveguide was designed first, starting with the procedure given in [5], p. 304. MMICAD [6] was then used to optimize the transformer further; the fringing capacitance at the steps was computed in MMICAD using the formulas in Marcuvitz [7], pp. 307-8. A listing of the MMICAD user-defined model for the waveguide step capacitance is given in the Appendix. The abrupt steps were then rounded as they would be if machined with an end-mill of diameter equal to the waveguide height (0.050" for WR-10) and QuickWave was used to determine the effect (small) of rounding the steps. The transformer itself has $|S_{11}| < -32$ dB across the waveguide band. The complete Y-junction was then formed by adding two E-plane bends to the large end of the transformer. With a perfect cusp at the junction of the bends, QuickWave simulation indicates $|S_{11}| < -31$ dB measured at the small end of the transformer — this is somewhat dependent on the length of square waveguide between the transformer and the bends. The realities of fabrication require the cusp to be truncated at a finite thickness, and versions A and B with cusps truncated at different widths were re-optimized by varying the length of the square waveguide section. Figure. 13 compares the measured and simulated results for version A.

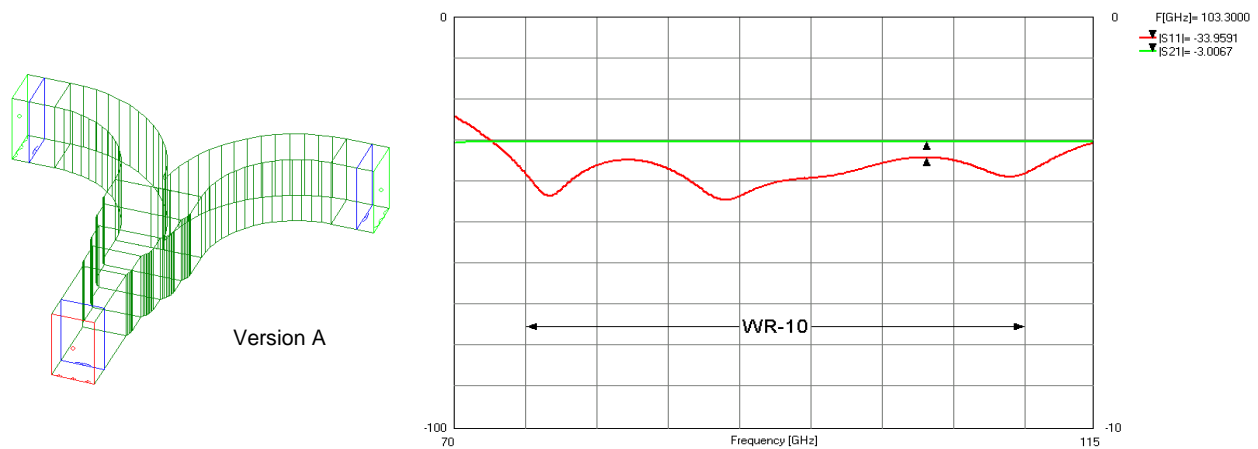


Fig. 9. WR-10 E-plane Y-junction, version A, with the cusp truncated at a width of 0.0020". QuickWave simulation of $|S_{11}|$ (dB) and $|S_{21}|$ (dB).

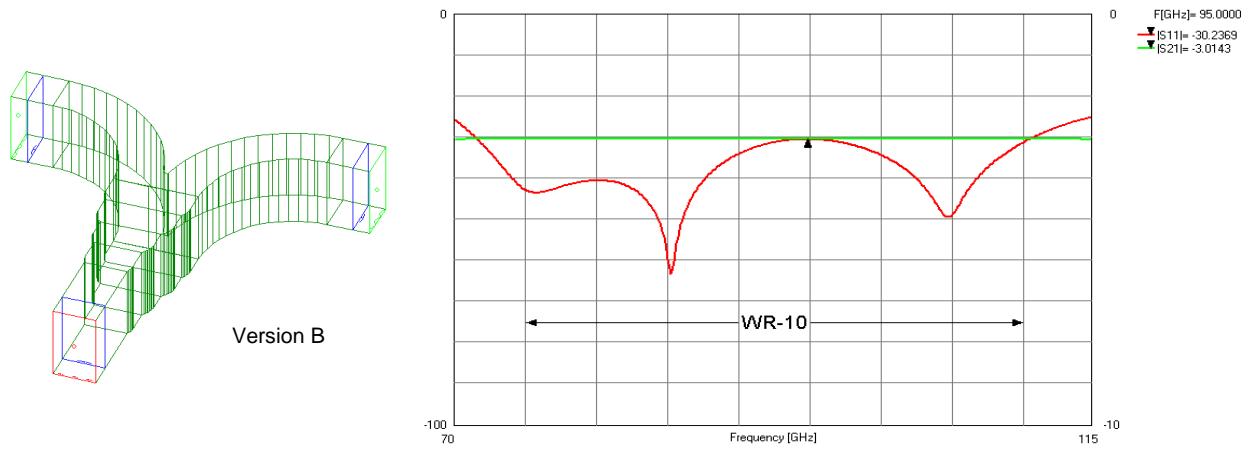


Fig. 10. WR-10 E-plane Y-junction, version B, with the cusp truncated at a width of 0.0057" . QuickWave simulation of |S11| (dB) and |S21| (dB).

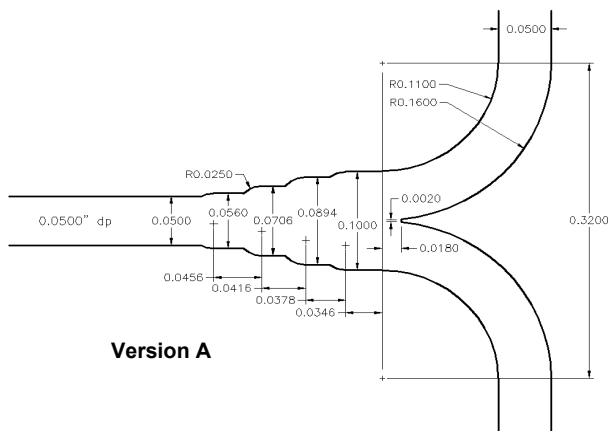


Fig. 11. Dimensions of WR-10 E-plane Y-junction, version A.

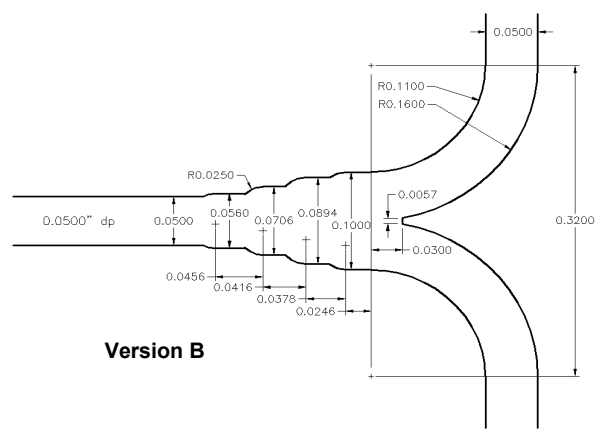


Fig. 12. Dimensions of WR-10 E-plane Y-junction, version B.

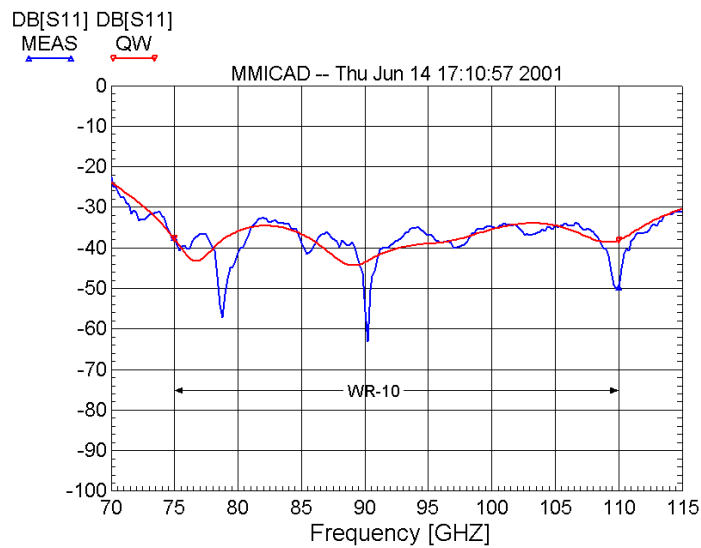


Fig. 13. Comparison of measured and simulated results for version A of the Y-junction.

The results of EM simulation using QuickWave are shown in Fig. 15. It is seen that $|S_{11}| < -21$ dB across the 75-110 GHz waveguide band.

The design is relatively tolerant to small errors in dimensions. Figure. 16 shows the effect of increasing the width of the substrate by 1 mil to fill the channel completely. The rise in $|S_{11}|$ towards 115 GHz (outside the normal waveguide band) is caused by a resonance in the odd mode of the suspended stripline — see Fig. 17. The frequency of this resonance also decreases as the height of the channel above the center conductor is increased; then less energy propagates in the air and more in the quartz, resulting in a higher effective relative dielectric constant for that mode.

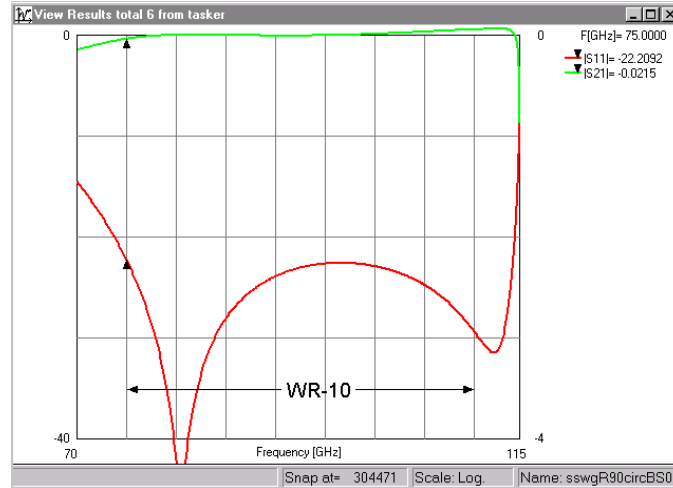


Fig. 16. QuickWave simulation of $|S_{11}|$ and $|S_{21}|$ (dB) for the waveguide to quartz suspended stripline transducer with the substrate width increased by 1 mil to fill the channel.

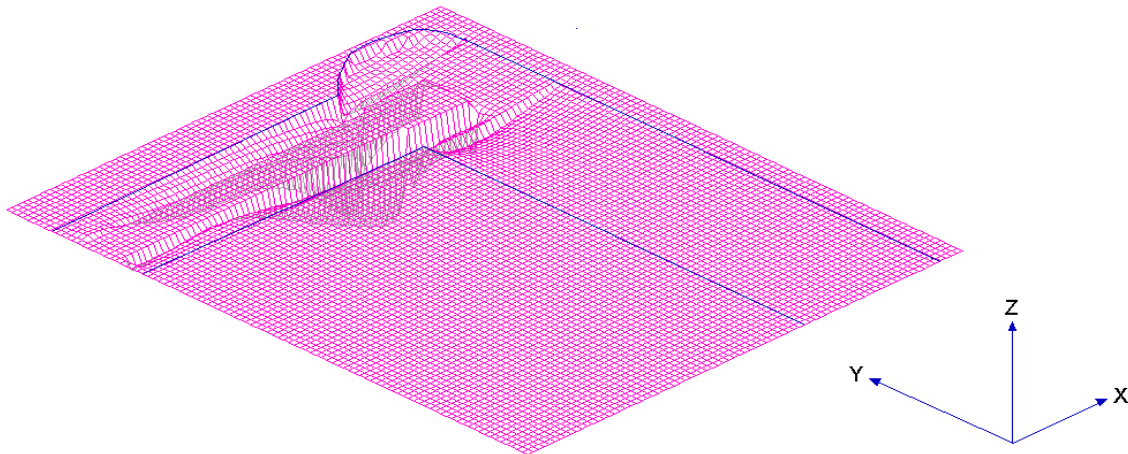


Fig. 17. QuickWave simulation of the E-field in the y -direction, showing the (out-of-band) odd-mode resonance in the suspended stripline.

5. Discussion

The waveguide elements described here are all in WR-10 to facilitate measurement with an HP8510 vector network analyzer. Scaling to other waveguide sizes with the same 2:1 aspect ratio is simple: all dimensions are modified by the factor (width of waveguide)/(width of WR-10).

E-plane split-block components with full symmetry about the plane of the split have no currents across that plane and will not be affected if contact between the two half-blocks is imperfect or if there is a small gap. However, the H-plane bend and the waveguide to suspended stripline transducer described here are asymmetrical about the plane of the split and may suffer from additional loss or even sharp resonances if there is poor contact or a gap between the halves. This problem has been investigated by Hesler [10, 11] who finds that a periodic array of short metal buttons machined into one half of the split block suppresses gap currents and almost completely eliminates resonances and excess loss.

The choice of waveguide flanges can significantly affect the performance of interconnected waveguide component and the ease with which they can be assembled properly. This is discussed in [12]. Flat waveguide flanges (*i.e.*, with no central boss) are the most practical choice for split-block waveguide components, and the mating waveguides should have flat or anti-cocking flanges.

6. Acknowledgment

The author thanks G. Ediss for finding the error in the parentheses in the Marcuvitz equation for the capacitance of a step in the height of a rectangular waveguide.

7. References

- [1] S. M. X. Claude, C. T. Cunningham, A. R. Kerr and S.-K. Pan, "Design of a Sideband-Separating Balanced SIS Mixer Based on Waveguide Hybrids," ALMA Memo No. 316, 16 Aug 2000. <http://www.alma.nrao.edu/memos/html-memos/alma316/memo316.pdf>.
- [2] S. Srikanth and A. R. Kerr, "Waveguide Quadrature Hybrids for ALMA Receivers," ALMA Memo 343, 11 Jan 2001. <http://www.alma.nrao.edu/memos/html-memos/alma343/memo343.pdf>.
- [3] A. R. Kerr and N. Horner, "A Broadband In-Phase Waveguide Power Divider/Combiner," ALMA Memo #325, 10 Oct 2000. <http://www.alma.nrao.edu/memos/html-memos/alma325/memo325.pdf>
- [4] QuickWave FDTD EM simulator, QWED s.c., Zwycieczów 34/2, 03-938 Warszawa, Poland.
- [5] G. L. Matthaei, L. Young, E. M. T. Jones, *Microwave Filters, Impedance-Matching Networks, and Coupling Structures*, New York: McGraw-Hill, 1964.
- [6] MMICAD microwave circuit analysis and optimization program, Optotek, Ltd., Ontario, Canada K2K-2A9.
- [7] N. Marcuvitz (ed.), *Waveguide Handbook*, MIT Rad. Lab. Series, vol. 10, New York: McGraw-Hill, 1951
- [8] A. R. Kerr, S.-K. Pan, S. Whiteley, M. Radparvar, and S. Faris, "A Fully Integrated SIS Mixer for 75-110 GHz," *IEEE Int. Microwave Symp. Digest*, pp. 851-854, May 1990.
- [9] A. R. Kerr, S.-K. Pan, A. W. Lichtenberger and D. M. Lea, "Progress on Tunerless SIS Mixers for the 200-300 GHz Band," *IEEE Microwave and Guided Wave Letters*, vol. 2, no. 11, pp. 454-456, Nov. 1992.
- [10] J. Hesler, "A Photonic Crystal Joint (PCJ) for Metal Waveguides," *2001 IEEE International Microwave Symposium Digest*, pp. 783-786, May 2001.
- [11] J. Hesler, "A Photonic Crystal Joint (PCJ) for Metal Waveguides," submitted to *IEEE Trans. Microwave Theory Tech.*, June 2001.
- [12] A. R. Kerr, E. Wollack, and N. Horner, "Waveguide Flanges for ALMA Instrumentation," ALMA Memorandum 278, 9 Nov. 1999. Available in pdf format at <http://www.mma.nrao.edu/memos/html-memos/alma278/memo278.pdf>.

APPENDIX — A MMICAD model for the capacitance of a symmetrical change of height of a rectangular waveguide

The element STEP represents the capacitance at a symmetrical change of height of a rectangular waveguide from height b to b' . For compatibility with the other rectangular waveguide elements in MMICAD, the definition of the waveguide characteristic impedance used in this model is:

$$Z_0 = 377 \frac{\pi b}{2 a} \left[1 - \left(\frac{f_c}{f} \right)^2 \right]^{-\frac{1}{2}}$$

The capacitance of the waveguide step is calculated using Eq. 2(a) on p. 307 of Marcuvitz [7], which is accurate to 1% for $b/\lambda_g < 1$, where b is the height of the larger waveguide.

To use the element STEP, the main .ckt file must contain a line similar to:

```
INCLUDE D:\MMICADV2\MI SC\WGStepCap01.mdl
```

Dimensions are passed to the model from the .ckt file, which should contain a DIM statement in the GLOBAL block; e.g.:

```
GLOBAL
DIM FREQ=1e+009 RES=1 COND=1 CAP=1e-012 IND=1e-009 LNG=2.54e-005 TIME=1e-012
```

The element STEP can then be used within the CKT block as any other element, e.g.,

```
STEP 2 0 A0=A0 B0=B3 BP=B2
```

Listing:

```
! WGStepCap01.mdl A. R. Kerr 19 April 2001
! Ref. Marcuvitz, p. 307, Eq. 2a.
! Accuracy: 1% for BG < 1.
! Units: As defined in Global Dim statement.

! Arguments:      A0 = a = width of both w/g's
!                 B0 = b = height of larger w/g
!                 BP = b' = height of smaller w/g

CKT
MODVAR A0=1 B0=1 BP=1
!ocvar FC={100E9*2.998E-3/(2*A0*DI MLNG)}
!ocvar ZG={377*(pi/2)*(B0/A0)/((1-(FC/FREQ)^2)^0.5)} ! ohms
!ocvar Y0={(1/ZG)/DI MCOND} ! in global units
!ocvar AA={BP/B0} ! alpha
!ocvar DD={1-AA} ! del ta = 1-alpha
!ocvar L0={2.998e-3*1E11/FREQ} ! lambda_0 (m)
!ocvar LG={L0/((1-(L0/(2*A0*DI MLNG))^2)^0.5)} ! lambda_g (m)
!ocvar BG={B0*DI MLNG/LG} ! BG = b/l ambdag
!ocvar BGP={BG*AA} ! b' /l ambdag
!ocvar A11={(1+AA)/(1-AA)}
!ocvar G={(1-BG^2)^0.5}
!ocvar GP={(1-BGP^2)^0.5}
!ocvar A={A11^(2*AA)}*((1+G)/(1-G))-(1+3*AA^2)/(1-AA^2)}
!ocvar AP={A11^(2/AA)}*((1+GP)/(1-GP))+(3+AA^2)/(1-AA^2)}
!ocvar C={(4*AA/(1-AA^2))^2}
!ocvar BYO={2*BG*( &
(LN(((1-AA^2)/(4*AA))) * A11^(0.5*(AA+(1/AA)))))+2*((A+AP+2*C)/(A*AP-C^2)) &
+((BG/4)^2)*((1/A11)^(4*AA))*((5*AA^2-1)/(1-AA^2)+(4/3)*((AA^2)*C/A))^2 &
)}
!ocvar BC={BYO*Y0}
ADM 1 0 G=0 B=BC
def1p 1 step(A0 B0 BP)
```